DESY HERA 96-07 1996 and
in UM-HE-96-20 Ann Arbor 1996

The polarization at high energy in HERA*

D.P.Barber, K. Heinemann, G. Hoffstätter×, and M. Vogt
DESY, 22603 Hamburg, Fed. Rep. Germany
× Inst. App. Physics, 64289 Darmstadt, Fed. Rep. Germany

August 26, 1996

1 Introduction

In order to maximize the number of collisions of stored particles in a storage ring system one tries to maximize the total number of particles in the bunches and tries to minimize the emittances so that the particle distribution across phase space is narrow and the phase space density is high. Furthermore, the beam should ideally be at equilibrium i.e. the phase space distribution should be periodic in the machine azimuth.

If, in addition, the beam is spin polarized, one requires that the polarization is high and in equilibrium. The polarization state of a spin 1/2 stored beam at equilibrium is defined by the phase space density distribution, the *value* of the equilibrium polarization at each point in phase space, and the *direction* of the equilibrium polarization at each point. Once we know these three functions we have a complete specification of the polarization state of the beam.

The maximizing of the polarization of the ensemble implies two conditions:

1. The polarization at each point in phase space should be high .

2. The equilibrium polarization vector at each point in phase space should be almost parallel to the average polarization vector of the beam.

Indeed, as we will show later, in the HERA proton ring it can happen that on average the equilibrium polarization vector deviates by tens of degrees from the average polarization vector of the beam. Thus even if each point in phase space were 100% polarized the average polarization could be limited to a value much smaller than 100%. The first condition requires that the source delivers high polarization and that the polarization is maintained during acceleration. The second condition is an intrinsic property of the arrangement of the magnets in the ring, the energy, and the optic. At the interaction points the average direction should, of course, be oriented according to the requirements of the experiments. If it were to be demonstrated that the ring and the optic do not permit a high parallelism, there would be little point in striving to fulfill condition 1.

This chapter is an extract from [1]. It deals with a perfectly aligned machine and can only serve to give a first impression. Much of the background has been covered in several other reports [2, 3, 4, 5, 6] and they should be consulted for mathematical details. Furthermore, an

*To appear in Acceleration of Polarized Protons to 820 GeV at HERA, UM HE 96–20

extensive study based mainly on long term spin-orbit tracking can be found in [7]. This also gives examples of spin-orbit motion for various Siberian Snake schemes.

2 The equilibrium polarization direction

Spin precession for particles traveling in electric and magnetic fields is described by the Thomas-Bargmann-Michel-Telegdi (T-BMT) equation [8, 9]:

$$\frac{d\vec{S}}{ds} = \vec{\Omega} \times \vec{S} \tag{1}$$

where $\vec{\Omega}$ depends on the electric and magnetic fields, the velocity and the energy. In magnetic fields at high energy equation (1) can be written as

$$\frac{d\vec{S}}{ds} = \frac{e\vec{S}}{mc\gamma} \times \{(1+G)\vec{B}_{||} + (1+G\gamma)\vec{B}_{\perp}\} \quad , \quad G = \left(\frac{g-2}{2}\right) \tag{2}$$

where $\vec{B}_{||}$ and $\vec{B}_{\perp}$ are the magnetic fields parallel and perpendicular to the trajectory, s is the arc length and the other symbols have the usual meanings. The gyromagnetic anomaly $G = \frac{g-2}{2}$ for protons is about 1.79. The full T-BMT equation contains terms depending on the electric field but these vanish if the electric field is parallel to the velocity. This is the case in radio frequency cavities in a first approximation. The T-BMT equation shows that in one turn around the design orbit of a flat storage ring a non-vertical spin precesses $a\gamma$ times. We call this latter quantity the 'naive spin tune' and denote it by ν_0. It gives the natural spin precession frequency in the vertical dipole fields of the ring. At 820 GeV, ν_0 is about 1557. The 'naive spin tune' is to be distinguished from the 'real spin tune' which must be used for calculations in rings with exotic magnet elements.

In horizontally bending dipoles, spins precess only around the vertical field direction. The quadrupoles have vertical and horizontal fields and therefore additionally cause the spins to precess away from the vertical direction. The strength of the spin precession and the precession axis in machine magnets depends on the trajectory and the energy of the particle. Thus in one turn around the ring the effective precession axis can deviate from the vertical and will depend on the initial position of the particle in six dimensional phase space. From this it is clear that if an equilibrium spin distribution exists, i.e. if the polarization vector at every phase space point is periodic in the machine azimuth, it will vary across the orbital phase space.

We denote the polarization at each point $\vec{z}$ in six dimensional phase space and at azimuth θ by $\vec{\mathcal{P}}(\vec{z},\theta)$. Since the T-BMT equation is linear in the spin, $\vec{\mathcal{P}}(\vec{z},\theta)$ obeys the T-BMT equation [10] which we now write in the form

$$\frac{d\vec{\mathcal{P}}}{d\theta} = \vec{\Omega}(\vec{z},\theta) \times \vec{\mathcal{P}} \; . \tag{3}$$

Because equation (3) describes precession, $|\vec{\mathcal{P}}(\vec{z},\theta)|$ is constant along a phase space trajectory.

At equilibrium, $\vec{\mathcal{P}}(\vec{z},\theta)$ not only obeys the T-BMT equation, but it is also periodic in θ. We write the equilibrium $\vec{\mathcal{P}}$ as $\vec{\mathcal{P}}_{eq}$ and we denote the unit vector along $\vec{\mathcal{P}}_{eq}(\vec{z},\theta)$ by $\vec{n}(\vec{z},\theta)$. Obviously $\vec{n}$ also obeys equation (3) and thus behaves like a spin. The vector $\vec{n}$ was first introduced by Derbenev and Kondratenko [11] in the theory of radiative electron polarization. By its definition the field of equilibrium spin directions in phase space does not change from turn

to turn when particles propagate through the accelerator. However, after each turn individual particles find themselves at new positions in phase space. Thus the periodicity condition implies that when a particle at an initial phase space point $\vec{z}_i$ is transported to a final point $\vec{z}_f$ during one turn around the storage ring we have

$$\underline{R}(\vec{z}_i, \theta)\vec{n}(\vec{z}_i, \theta) = \vec{n}(\vec{z}_f, \theta) \ . \tag{4}$$

where $\underline{R}(\vec{z}_i, \theta)$ is the orthogonal spin transport matrix for one turn on that orbit.

Clearly, it is very important to have accurate and efficient methods for calculating $\vec{n}(\vec{z}, \theta)$. Note that $\vec{n}(\vec{z}, \theta)$ is usually not an eigenvector of the spin transfer matrix at some phase space point since the spin of a particle changes after one turn around the ring, but the eigenvector would not change.

We expect that the spins would reach their equilibrium distribution simply as a result of the adiabatic acceleration process [3].

3 The HERA lattice

In this section we describe the model for the HERA ring used in our calculations.

The HERA ring has a circumference of about 6.335 kilometers. There are a total of one hundred FODO cells in the arcs and the phase advance per cell is 90 degrees in both planes. In anticipation of field nonlinearities due to persistent currents in the superconducting magnets, multipole correction windings are built into many of the magnets. For the calculations presented here nonlinear fields and skew fields are ignored. The orbit motion is linearized.

A further aspect of the HERA proton ring and one that has a totally nontrivial implications for spin motion is that there are sets of interleaved vertical and horizontal bends on each side of the North, South, and East interaction points. These serve to adjust the height of the proton ring to that of the electron ring at the collision points. Coming from the arc, a proton is first bent 5.74 milliradians downwards, then 60.4 milliradians towards the ring center and finally the orbit is made horizontal by a 5.74 milliradians upward bend. The structure is repeated with interchanged vertical bends on the far side of the interaction point at the entrance to the arc.

It is easy to see that with $a\gamma \approx 1557$ the interleaved vertical and horizontal bends cause a massive disturbance to the spin motion. In a perfectly aligned ring without vertical bends the equilibrium spin direction on the design orbit, $\vec{n}_0 = \vec{n}(0, \theta)$ is vertical. With vertical bends $\vec{n}_0$ is no longer vertical and strongly energy dependent.

In the West area there is no interaction point for collisions with electrons and positrons. So there are no vertical bends. Our calculations are based on the 1996 luminosity optic. This optic and the magnets are not symmetric with respect to the center of the West area owing to the presence of the HERA-B experiment and beam dump magnets. However, in these calculations the vertical bump associated with the beam dump mechanism is switched off so that the design orbit is horizontal across the whole West area.

The betatron tunes are $Q_x \approx 31.279$ and $Q_z \approx 32.273$. The synchrotron tune at full energy is about 0.000625. For these calculations the invariant one sigma emittance ϵ_σ is taken to be $4\pi \cdot 10^{-6}$ meter radians in both planes; this value is obtained under optimum conditions. The invariant one sigma emittance is defined to be $\gamma v/c$ times the area of an upright ellipse passing through the phase space point ($x = \sigma$,x'=0). This area $\epsilon_\sigma/(\gamma v/c)$ is equal to $\pi\sigma^2/\beta$; β is the optical beta function, γ is the relativistic factor, and v/c is the velocity. For Gaussian beams the one sigma ellipse contains 39% of the beam in each dimension. The fractional ('1 sigma')

energy spread is about $5 \cdot 10^{-5}$. However, synchrotron oscillations are not considered in this report.

4 Computational techniques

4.1 Straightforward polarization tracking

One can try to get information about the spread of the equilibrium spin directions over phase space by tracking a completely polarized beam for many turns. This is illustrated in figure 1. There are no geometrical distortions and the vertical bends are turned off so that the simulation represents a perfectly aligned flat ring. Particles at 100 different phases on a 1 sigma vertical phase space ellipse and zero longitudinal and horizontal emittance have been tracked through HERA for 600 turns while the beam was initially 100% polarized parallel to $\vec{n}_0$. Similar kinds of tracking results have been presented in [7]. The polarization of the ensemble is defined as the average across the phase space of the unit spin vectors. We see that the polarization oscillates wildly. This polarization distribution is obviously not an equilibrium distribution and this implies that the $\vec{n}$-axes are widely spread out away from $\vec{n}_0$. The bold horizontal line is the turn by turn polarization obtained when each spin is initially set parallel to $\vec{n}(\vec{z},\theta)$ (calculated using the code SPRINT–see below) at its phase space position $\vec{z}$. Now the averaged polarization stays constant at 0.765. This latter value is consistent with the fact that the average opening angle is about 40 degrees. Therefore, by starting simulations with spins parallel to the $\vec{n}$-axis one can perform a much cleaner analysis of beam polarization in accelerators. In effect one is now able to study the effect of spin perturbations (for example due to field noise, beam-beam effect etc) by searching for small deviations away from the 'stationary state' of the beam instead of having to detect long term drifts in a strongly fluctuating average polarization.

4.2 The linear (SLIM) theory

A well established and often justified procedure is to linearize the orbit motion. A spin can be parameterized by two angles describing its tilt away from $\vec{n}_0$. Under some circumstances one can additionally linearize with respect to these angles. This is the basis of the code SLIM for calculating electron spin diffusion [12]. $\vec{n}$ can similarly be calculated in linear approximation [13]. However, since $\vec{n}$ in a very high energy accelerator such as HERA can be widely spread out away from $\vec{n}_0$, the two angles can be large. In this case this linearization is not justified. Nevertheless the technique has been used to get a first indication that the equilibrium polarization in the HERA proton ring could be limited due to a large spread of the opening angle [3].

4.3 Nonlinear normal form analysis

Nonlinear normal form theory provides solutions of equation (4) beyond first order by computing the Taylor expansion of $\vec{n}(\vec{z},\theta)$ with respect to $\vec{z}$. Theoretically the evaluation order is not limited, but computational errors typically limit the normal form approach to fifth order. Experience has shown that except when the spread of polarization directions is small, this method diverges and a nonperturbative method is needed. When the spread has already been reduced by some means, normal form analysis has been successfully applied in the filtering method mentioned below [4].

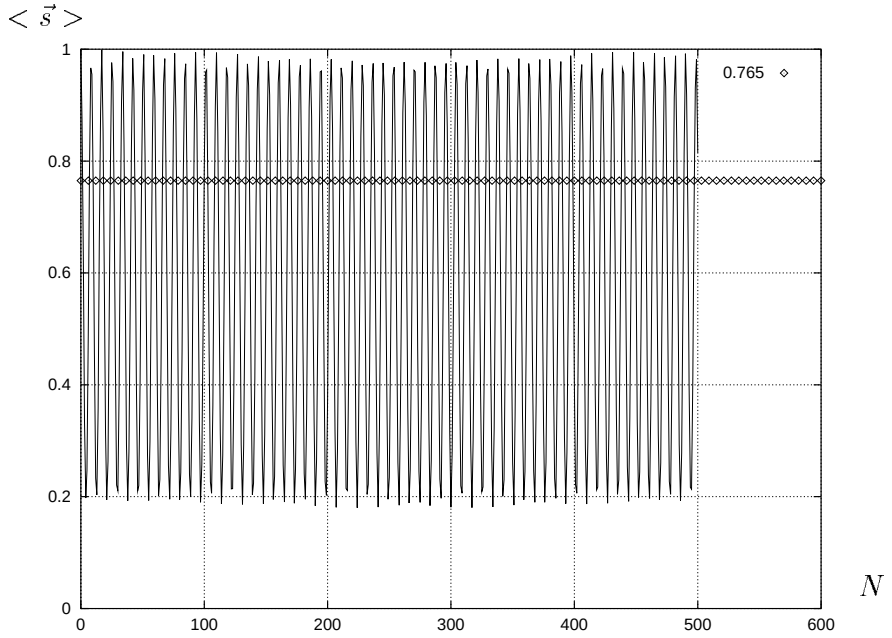

Figure 1: Propagation of a beam that is initially completely polarized parallel to $\vec{n}_0$ leads to a fluctuating average polarization. For another beam that is initially polarized parallel to the periodic spin solution $\vec{n}$ the average polarization stays constant, in this case equal to 0.765.

4.4 Stroboscopic averaging

However, in order to handle the general case we have developed a new method for obtaining $\vec{n}$ called stroboscopic averaging [5]. It is based on multi-turn tracking and the averaging of a special choice of the spin viewed stroboscopically from turn to turn. Since this innovative approach only requires tracking data from *one particle*, it is fast and very easy to implement in existing tracking codes. Probably the main advantage over other methods is the fact that stroboscopic averaging does not have an inherent problem with either orbit or spin orbit resonances due to its nonperturbative nature. This allows the analysis of the periodic spin solution close to resonances. This algorithm has been implemented in the program SPRINT [5]. This is the code used to calculate the initial $\vec{n}$-axes needed to propagate the equilibrium distribution in figure 1.

The stroboscopic average has a very simple physical interpretation which illustrates its practical importance. If a particle beam is approximated by a phase space density, disregarding its discrete structure, then we can associate an arbitrary spin field $\vec{\mathcal{P}}(\vec{z}, \theta_0)$ with the particle beam at the azimuth θ_0. If one installs a point like 'gedanken' polarimeter at a phase space point $\vec{z}_0 = \vec{z}(\theta_0)$ and azimuth θ_0, then this polarimeter initially measures $\vec{\mathcal{P}}(\vec{z}_0, \theta_0)$. When the particle beam passes the azimuth θ_0 after one turn around the ring, the polarimeter measures

$$\underline{R}(\vec{z}(\theta_0 - 2\pi), \theta_0 - 2\pi) \cdot \vec{\mathcal{P}}(\vec{z}(\theta_0 - 2\pi), \theta_0) \ . \tag{5}$$

After the beam has traveled around the storage ring a large number of times and the polarization has been measured whenever the beam passed the 'gedanken' polarimeter, one averages over the different measurements to obtain $< \vec{\mathcal{P}} >$. In [5] it has been proved that this average is parallel to $\vec{n}(\vec{z}_0, \theta_0)$. If the particles of a beam are polarized parallel to $\vec{n}(\vec{z}, \theta_0)$ at every phase

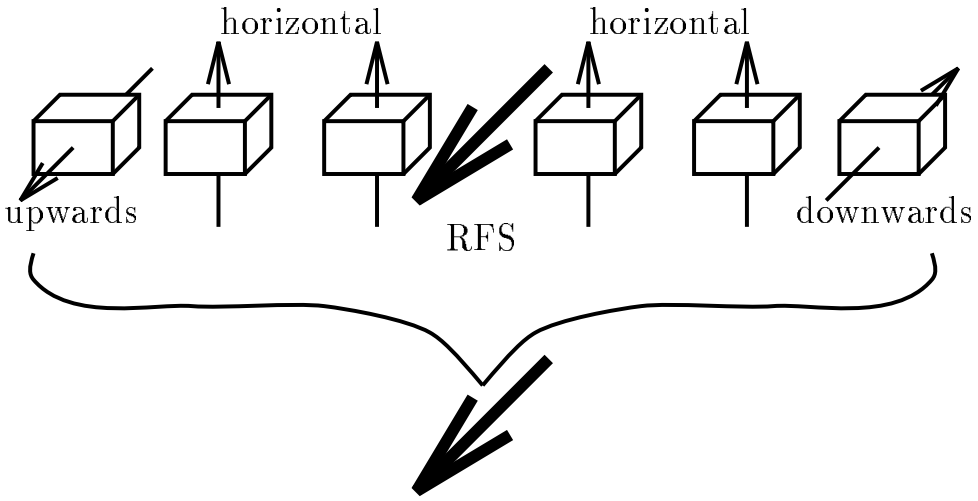

Figure 2: A schematic layout of the interleaved horizontal and vertical bending magnets near the North, South and East interaction points of HERA. The arrows indicate the orientation of the precession axes. If one places a radial Siberian Snake (indicated by the thick arrow) at the midpoint of the four equal horizontal bends one obtains a radial Siberian Snake.

space point, then the spin field of the beam is invariant from turn to turn due to the periodicity property in equation (4). But in addition, even for beams which are not polarized parallel to $\vec{n}$, we see that the polarization observed at a phase space point $\vec{z}$ and azimuth θ_0 is still parallel to $\vec{n}(\vec{z}, \theta_0)$, if one averages over many measurements taken when the beam has passed the azimuth θ_0.

5 Limits to the polarization in HERA

This section describes calculations of the $\vec{n}$-axis for a perfectly aligned HERA.

As we pointed out above, the spin motion in HERA is complicated by the presence of interleaved vertical and horizontal bends. If we require that $\vec{n}_0$ is vertical in the arcs at all energies, the vertical bends must be compensated. One way to do this, proposed by V. Anferov [15], would be to insert a radial Siberian Snake at the midpoint of the 60.4 mrad horizontal bends (see figure 2). Owing to their special purpose, we will refer to these devices as ring flattening snakes (RFS). The complete magnet system spanning the vertical bends on one side of an interaction point then rotates spins by 180 degrees around the radial direction independently of the energy and therefore also behaves like a Siberian Snake. The spin rotation from the system on the upstream side of the interaction point compensates that from the downstream side so that the non-flat straight sections are transparent to spins on the closed orbit and $\vec{n}_0$ is vertical in the arcs. For the calculations presented here the vertical bends are switched off in the East corresponding to a geometry in which the proton beam remains at fixed height in the East area. Thus no RFS's are needed there. In the full report [1] the case of the non-flat East area is also considered. All snake-like elements are modeled by thin lenses which have no effect on the orbit and rotate all spins by 180 degrees independently of their positions in phase space. Clearly, at a later stage, realistic descriptions of snake fields will be needed.

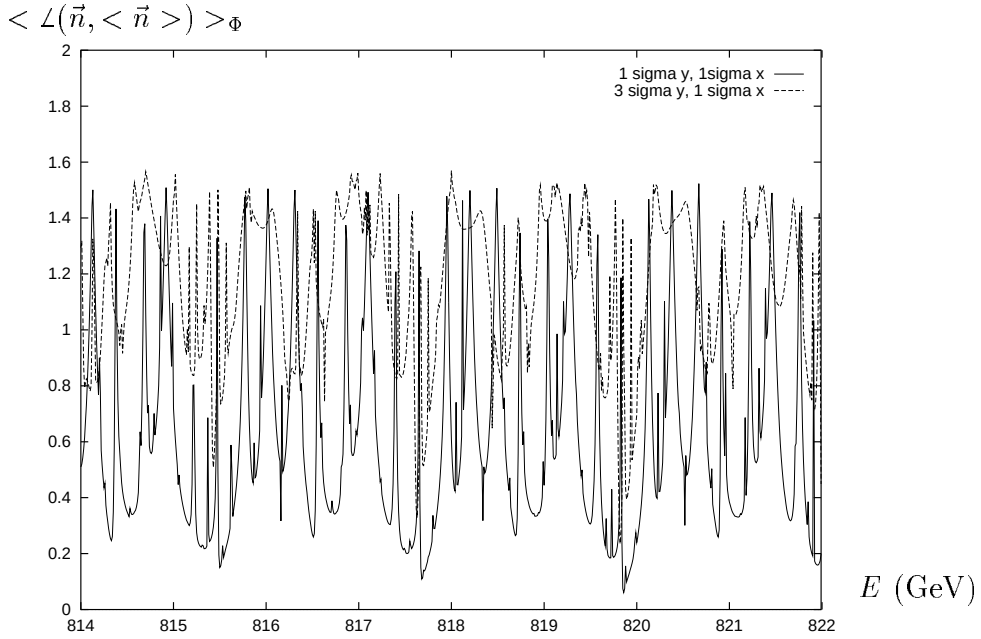

Figure 3: Average opening angle of the equilibrium polarization distribution for particle energies between 814 and 822 GeV with four ring flattening Siberian Snakes to make the North and the South straight sections spin transparent for particles on the closed orbit. The two curves refer to particles with one sigma in the horizontal direction and one or three sigma in the vertical direction respectively.

5.1 HERA without Siberian Snakes

Figure 3 (solid curve) shows the average angular deviation of $\vec{n}$ from its average (over the phase space) at the midpoint of the East interaction region for the layout just described and for particles distributed uniformly around the 1 sigma vertical and horizontal phase space ellipses. The calculation was made at *fixed* energies in the range 814–822 GeV and the angle is measured in radians. Synchrotron motion is not included. We see very strong variations of the opening angle with the minimum lying at about 60 mrad and the maximum at about 90 degrees. The maxima occur at the positions of the spin orbit resonances. Qualitatively similar curves are obtained at other positions in the ring. This curve is almost identical to that obtained when all vertical bends and the RFS's are switched off. The trained eye will detect a periodicity in the energy reflecting the approximate four fold symmetry of the ring. The number of resonance peaks would be smaller with exact four fold symmetry. It is clear from this figure that even in a perfectly aligned ring, acceptable polarization could be obtained only over a very restricted part of the energy range even if a completely polarized beam were delivered at high energy. The broken curve shows the average angular deviation of $\vec{n}$ from its average for particles distributed uniformly around the 3 sigma vertical and 1 sigma horizontal phase space ellipses.

5.2 HERA with Siberian Snakes

Siberian Snakes are not only essential for suppressing depolarization during acceleration but also help at fixed beam energy. In particular they are essential for suppressing spin flip effects

due to resonance crossing as the energies of individual particles execute (slow) synchrotron oscillations [7]. Note that we ignored synchrotron motion in the last subsection precisely because synchrotron motion in the absence of the snakes can destroy the polarization. Snakes also stabilize the spin motion due to betatron oscillation since the orbital tunes can be chosen so as not to coincide with the fixed real spin tune generated by properly chosen snake layouts. Figure 5 shows the average angular deviation of $\vec{n}$ for the RFS layout described above and for the same orbit amplitudes as in figure 3 but with a snake layout suggested by V. Anferov [15], and previously studied in a slightly modified form for a flat ring in [7](figure 51a). As shown in figure 4, there are snakes, with radial axes, near the vertical bends in the North and South, a snake with a radial axis near the midpoint of the West region, and a snake with a longitudinal axis near the midpoint of the East interaction region. The real spin tune is 1/2 independently of the energy and $\vec{n}_0$ is again vertical in the arcs and at the interaction points. No spin rotators have been included. The solid curve is for particles distributed uniformly around the 1 sigma vertical and 1 sigma horizontal phase space ellipses. Now we see that the dependence of the opening angle on energy is much smoother with a maximum in this energy range of about 0.72 radians and a minimum of about 0.3 radians. Even here, acceptable polarization could be obtained only over a restricted part of the energy range. The broken curve is for particles distributed uniformly around the 3 sigma vertical and 1 sigma horizontal phase space ellipses.

Figure 5 shows that installation of snakes is in itself not sufficient to ensure that an acceptable polarization is attainable. As a next step we therefore used the following automatic filtering method aimed at inspecting all possible combinations of four Siberian Snakes and eliminating choices which do not satisfy certain criteria. The procedure works as follows:

1. Find all snake combinations for the ring which was flattened by RFS's which lead to a spin tune of $\nu = 1/2$.

2. Compute the 1st order opening angle for the non-flat HERA proton ring and filter on small opening angles of the equilibrium spin distribution.

3. Compute the opening angle by 3rd and 5th order normal form theory for the snake combinations which are left after all these filters and filter on small opening angles if the normal form theory converges.

4. Compute the accurate equilibrium spin direction $\vec{n}$ with stroboscopic averaging.

When we only use Siberian Snakes with vertical, radial or longitudinal axes, the best parallelism in a polarized beam in HERA is achieved by a longitudinal snake in the East and vertical snakes close to the three other interaction points. The polarization distribution over the one and three sigma vertical phase space ellipses with 1 sigma in the horizontal direction calculated using SPRINT is displayed in figure 6. Now the $\vec{n}$-axes are more tightly bundled and beam of higher polarization can be stored in HERA. We display results for this case since they are the best found so far, in spite of the fact that this arrangement will probably not be chosen in practice, since the average polarization in the arcs is not vertical. At first sight one might suspect that this case is effectively equivalent to that with a single longitudinal snake and that vertical snakes would therefore not improve the spin motion. However this suspicion is not supported by our calculations. Other choices of Siberian Snakes have been suggested, for example a solution with 45° snakes in the North and South [17]. These suggestions exhibited an even more disadvantageous behavior for the equilibrium spin distribution.

Further optimization might improve the situation but there are several other effects which might have serious consequences for the storage of polarized protons.

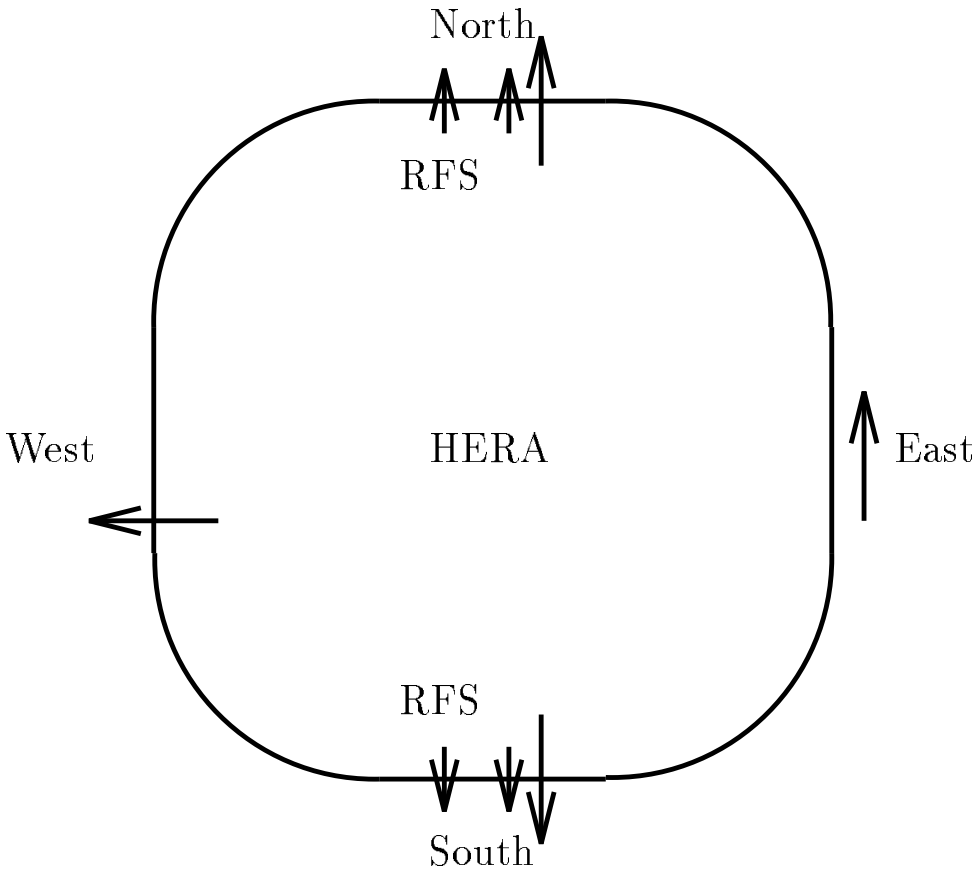

Figure 4: The placement of four spin flattener snakes to make the straight sections in the North and the South transparent to spins on the closed orbit and the placement of a longitudinal and three radial Siberian Snakes in HERA.

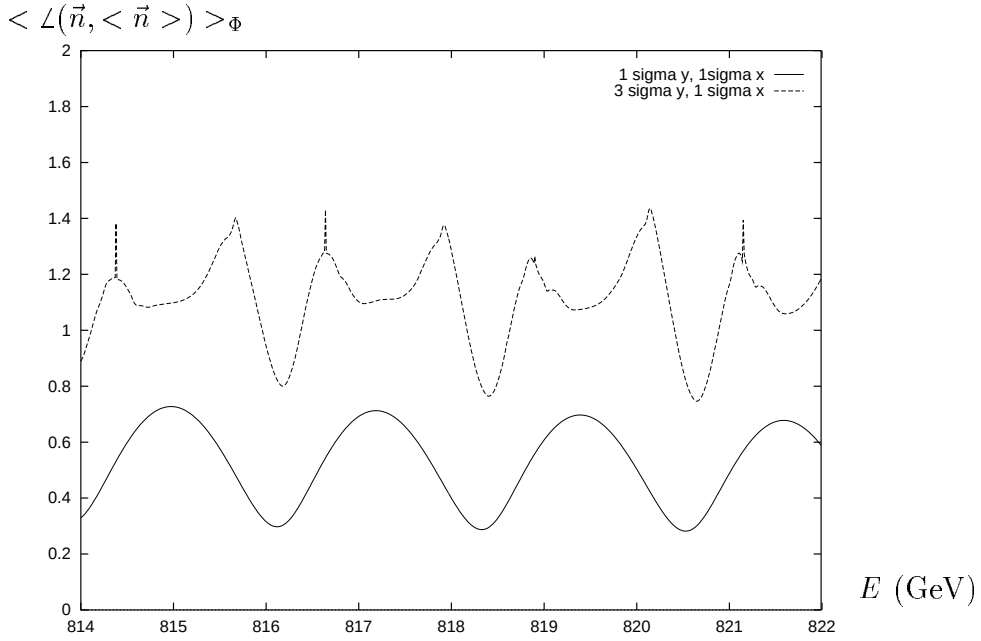

Figure 5: The average opening angle of the equilibrium spin distribution for energies between 814 and 822 GeV after the installation of the Siberian Snakes shown in figure 4. The two curves refer to particles with one sigma in the horizontal direction and one or three sigma in the vertical direction respectively.

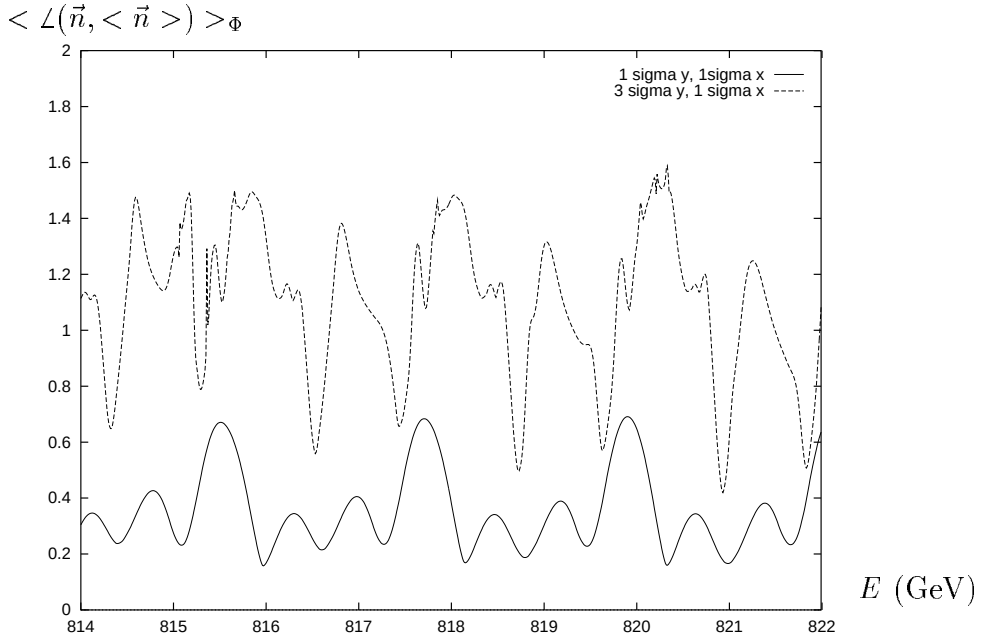

Figure 6: The average opening angle of the equilibrium spin distribution for energies between 814 and 822 GeV after the installation of the snake arrangement found by filtering. The two curves refer to particles with one sigma in the horizontal direction and one or three sigma in the vertical direction respectively.

6 Further investigations

Apart from the obvious need to find adequate and practical snake schemes, to decide the best way to realize the RFS's and to design and position the spin rotators needed to provide various $\vec{n}_0$ directions for the experiments at the interaction points, the following topics must be addressed.

1. Understand the effects of misalignments. Find cures. (The most important additional limitation to the polarization is likely to be the spread in the $\vec{n}$-axes caused by misalignments.)
2. Include linear and nonlinear synchrotron oscillations.
3. Determine the maximum allowed emittances.
4. Study the efficacy of the chosen snake scheme for controlling the spin 'equilibrium' during the adiabatic acceleration.
5. Determine the influence of the beam-beam effect.
6. Understand the influence of noise in power supplies.
7. Calculate with optical nonlinearities and optical coupling.
8. Evaluate the effect of intra-beam scattering, if any.
9. Investigate the relevance and feasibility of spin matching [14] and in particular the 'strong spin matching' proposed by K. Steffen [16].
10. Evaluate the advantages of increasing the symmetry of the ring and the optic.

Acknowledgement

We thank members of the SPIN Collaboration for useful discussions.

References

[1] D. P. Barber, K. Heinemann, G. H. Hoffstätter and M. Vogt. Limits to the equilibrium proton spin polarization at high energy in HERA. DESY Report in preparation.

[2] D. P. Barber. Prospects for polarized protons at HERA, In *International School of Nucleon Structure, 1st Course: The spin structure of the nucleon*, Erice, Sicily, August 1995. To be published by World Scientific Publishing Co. Ltd.

[3] D. P. Barber. Possibilities for polarized protons at HERA. In *Prospects of spin physics at HERA*, DESY–Zeuthen, August 1995. DESY Report 95–200, November 1995.

[4] G. H. Hoffstätter. Polarized protons in HERA. In *Proceedings of the DESY Accelerator Group Seminar,* St.Englmar, January 1996. DESY Report 96-05, May 1996.

[5] K. Heinemann and G. H. Hoffstätter. A tracking algorithm for the stable spin polarization field in storage rings using stroboscopic averaging. DESY Report 96–078, May 1996. Accepted for publication in Physical Review E.

[6] D. P. Barber, K. Heinemann, G. H. Hoffstätter and M. Vogt. The phase space dependent spin polarization direction in the HERA proton ring at high energy. In *The Proceedings of the 1996 European Particle Accelerator Conference*, Sitges, Spain, May 1996.

[7] V. Balandin, N. Golubeva, and D. P. Barber. Studies of the behaviour of proton spin motion in HERA-p at high energies. DESY Report M-96-04, February 1996.

[8] L. Thomas. The kinematics of an electron with an axis. *Philosophical Magazine*, **3**, 1 (1927).

[9] V. Bargmann, L. Michel and V. L. Telegdi. Precession of the polarization of particles moving in a homogeneous electromagnetic field. *Phys.Rev.Lett.,* **2**, 435 (1959).

[10] K. Heinemann. Thesis in preparation.

[11] Ya. S. Derbenev and A. M. Kondratenko. Diffusion of particle spins in storage rings. *Sov. Phys. JETP*, **35**, 230 (1972).

[12] A.W. Chao. Evaluation of radiative spin polarization in an electron storage ring. *Nuclear Instruments and Methods*, **180**, 29 (1981).

[13] D.P. Barber, K. Heinemann, and G. Ripken. A canonical 8-dimensional formalism for classical spin-orbit motion in storage rings. II Normal forms and the n-axis. *Zeitschrift für Physik*, **C64**, 143 (1994).

[14] D.P. Barber, et al. A solenoid spin rotator for large electron storage rings. *Particle Accelerators*, **17**, 243 (1985).

[15] V. Anferov. Private communication. See also the Chapter 10.

[16] K. Steffen. Strong spin matching with and without snakes: a scheme for preserving polarization in large ring accelerators. *Particle Accelerators*, **24**, 45 (1988).

[17] E. Courant. Private communication.